Electrical resistivity of single crystals of LaFeAsO under applied pressure

C. A. McElroy, J. J. Hamlin, B. D. White, S. T. Weir, Y. K. Vohra, and M. B. Maple

Phys. Rev. B **90**, 125134 — Published 19 September 2014

DOI: 10.1103/PhysRevB.90.125134

Electrical Resistivity of Single Crystals of LaFeAsO Under Applied Pressure

C. A. McElroy,[1,2] J. J. Hamlin,[1,2,*] B. D. White,[1,2] S. T. Weir,[3] Y. K. Vohra,[4] and M. B. Maple[1,2]

[1]*Department of Physics, University of California, San Diego, La Jolla, California 92093, USA*
[2]*Center for Advanced Nanoscience, University of California, San Diego, La Jolla, California 92093, USA*
[3]*Condensed Matter and Materials Division, Lawrence Livermore National Laboratory, Livermore, California 94550, USA*
[4]*Department of Physics, University of Alabama at Birmingham, Birmingham, Alabama 35294, USA*

(Dated: September 8, 2014)

Measurements of electrical resistivity under applied pressure were performed on single crystalline samples of LaFeAsO grown in a molten NaAs flux. We observe a smooth suppression of spin-density wave order under nearly hydrostatic applied pressures up to 2.6 GPa and in quasi-hydrostatic pressures up to 14.7 GPa. Similar to some of the other reports on single and polycrystalline samples of LaFeAsO, these crystals exhibit a resistivity that increases as temperature is lowered. By fitting an Arrhenius law to the the semiconducting-like temperature dependence of the electrical resistivity, we extract an energy gap that is suppressed with pressure and vanishes near 10 GPa. This is accompanied by the emergence of a metallic temperature dependence of the electrical resistivity. A similar behavior is also observed in diamond anvil cell experiments carried out to $\sim 37\,\mathrm{GPa}$. Complete transitions to a bulk superconducting phase are not observed in any of the experiments.

PACS numbers: 71.30.+h, 74.70.Xa, 74.62.Fj

I. INTRODUCTION

The discovery of superconductivity in fluorine-substituted layered pnictide compounds LaFePO[1] and LaFeAsO[2] has driven significant theoretical and experimental interest in these and many other members of the diverse taxonomy of iron pnictide and chalcogenide compounds.[3–6] As a function of chemical substitution or applied pressure, the phase diagrams of these materials exhibit a rich interplay of different phenomena, including structural transitions, commensurate and incommensurate spin-density wave (SDW) ordering, and high temperature superconductivity.[5–13]

In several iron-based materials, the appearance of superconductivity occurs following a smooth suppression of SDW order. Among the materials in which such a continuous suppression is observed are, *e.g.*, $BaFe_2As_2$ (under both chemical substitution and applied pressure)[14] and fluorine-substituted $CeFeAsO_{1-x}F_x$.[15] By contrast, in the $LaFeAsO_{1-x}F_x$ system μSR and Fe Mössbauer spectroscopy measurements reveal that the structural and SDW transitions abruptly undergo a first-order phase transition near $x = 0.05$.[3] For $x > 0.05$, SDW order is absent and superconductivity emerges such that there is no overlap between the two phases.[2] However isovalent phosphorus substitution ($LaFeAs_{1-x}P_xO$) appears to induce a continuous suppression of SDW order, with some overlap between the magnetically-ordered and superconducting phases.[16]

Characterizing the evolution of SDW order under applied pressure provides important complementary information on the interplay of superconductivity and magnetism in ZrCuSiAs-type materials. The pressure-temperature phase diagram of the undoped parent compound LaFeAsO was previously examined by Okada *et al.*[17] using polycrystalline samples. The resulting phase diagram appeared to indicate a smooth suppression of the SDW and a region of overlap between the SDW and superconductivity. This suggests that the phase diagram of LaFeAsO under applied pressure has a different character than that of the temperature-chemical concentration phase diagram obtained from studies of fluorine substitution for oxygen.[2] However, the feature in the electrical resistivity data associated with the SDW order in that study was broad and difficult to distinguish with accuracy at high pressures.

In this paper, we report the results of high pressure electrical resistivity measurements on single crystals of LaFeAsO. These single crystals exhibit well-resolved resistive anomalies at the SDW transition to higher pressures than their polycrystalline counterparts, providing an opportunity to more precisely characterize T_{SDW} as a function of pressure. Under nearly hydrostatic pressures, T_{SDW} extrapolates to zero near 6 GPa. Similar to some of the other reports on both single and polycrystalline samples of LaFeAsO, these crystals exhibit an electrical resistivity that increases as temperature is lowered.[18] By assuming an activated Arrhenius-type behavior, we have extracted an energy gap from the temperature dependence of the electrical resistivity ρ. This gap extrapolates to zero at 10 GPa, near the same pressure region where the electrical resistivity shows a crossover to a metallic behavior where $d\rho/dT > 0$. At pressures above 10 GPa, small downturns in the electrical resistivity, consistent with an incomplete superconducting transition, are evident. However, the samples do not appear to exhibit bulk superconductivity to pressures as high as $\sim 37\,\mathrm{GPa}$.

II. EXPERIMENTAL DETAILS

Single crystals of LaFeAsO were grown using a molten NaAs flux[19] and characterized with powder x-ray diffraction, magnetization, and specific heat measurements. The samples were confirmed to have the ZrCuSiAs-type crystal structure with lattice parameters $a = b = 4.0334$ Å and $c = 8.7910$ Å. The tetragonal to orthorhombic structural phase transition T_{ST} was observed near 140 K and the SDW order occurs near $T_{SDW} \simeq 120$ K as reported in a previous study.[18] Differences in the measured lattice parameters of our single crystals[18]

compared with those reported in earlier studies[20] suggests the possible incorporation of impurities during crystal growth either from the tantalum crucible or the sodium in the flux itself. In our previous study of LaFeAsO single crystals, we confirmed the stoichiometry via energy dispersive x-ray spectroscopy but also noted the presence of a La_3TaO_7 impurity phase (approximately 2% molar fraction). The behavior of materials within this genus of the iron-pnictide family has, in some cases, been shown to be very sensitive to doping, impurities, and oxygen vacancies.[5,13,21,22] In our earlier study[4,6] on these samples, we measured lower transition temperatures, T_{SDW} and T_{ST}, relative to results from measurements of polycrystals and other single crystals at ambient pressure.[9,23] We compare the results of ambient pressure measurements on our single crystals of LaFeAsO to similar measurements discussed by Yan *et al.* in the Results and Discussion section of this paper.[19]

Electrical resistivity measurements under applied pressures up to approximately 2.6 GPa were made using a standard four-wire technique in a piston cylinder cell (PCC). Equal parts of isoamyl alcohol and n-pentane were used as the pressure transmitting medium.[24] The applied pressure was always adjusted at temperatures above the melting point of the pressure medium in order to ensure nearly hydrostatic conditions. In-situ measurements of the pressure within the sample space were made inductively using the well-characterized superconducting transition of high-purity Sn as a manometer.[25]

The electrical resistivity under applied pressures up to 14.7 GPa was measured using a quasi-hydrostatic Bridgman anvil cell (BAC).[26] The sample space is constructed using a pyrophyllite gasket with steatite as the pressure-transmitting medium. This space is pressurized between two tungsten-carbide anvils which press platinum wires on to both the sample and the Pb manometer for electrical contact. The small strip of lead functioned as a manometer by measuring its well-characterized superconducting transition resistively.[27]

The higher pressure range (up to approximately 36 GPa) was investigated using a diamond anvil cell (DAC). This technique uses two diamonds as anvils between which the sample, suspended in a pressure transmitting medium of steatite and constrained by a MP35N gasket, is compressed.[28] One of the anvils is a designer diamond in which tungsten leads are deposited directly onto the original diamond and then encapsulated within a layer of epitaxially grown diamond that serves to protect and insulate the leads from the gasket.[29,30] The culet of the designer diamond anvil is then polished to expose the tungsten leads within the gasket and allow electrical transport measurements to be performed. In-situ measurements of the pressure within the cell were performed by measuring the fluorescence spectrum of a small piece of ruby while exciting it with light from a 472 nm laser. The evolution of this fluorescence spectra is well known and provides a convenient, measurement of the pressure within the sample space.[31]

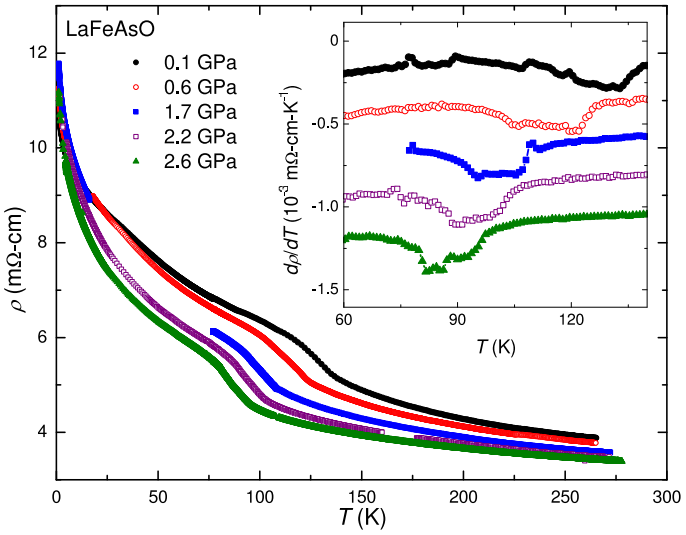

FIG. 1: Electrical resistivity ρ vs. temperature T measured in quasi-hydrostatic applied pressures up to 2.6 GPa. Spin-density wave order is suppressed with increasing pressure from approximately 134 K to 80 K. The inset shows the first derivative of the electrical resistivity with respect to temperature with each set of data offset by a constant value.

III. RESULTS AND DISCUSSION

At ambient pressure, $\rho(T)$ of these single crystals exhibits semiconducting-like behavior in which $d\rho/dT < 0$ over the entire range of temperatures measured.[18] This behavior for $\rho(T)$ has been observed in other ambient-pressure measurements of single-crystalline samples (see the supplemental material of Ref. 19). On the other hand, it contrasts with measurements on polycrystalline samples,[17] which have consistently shown $d\rho/dT > 0$ at temperatures just below T_{SDW} and $d\rho/dT < 0$ at the lowest temperatures. While some potential explanations for this difference have been offered in a study of samples grown using a molten KI flux,[20] and may explain the behavior of our single crystals, a precise explanation for this difference in our samples grown using a NaAs flux will require further study. It is worth pointing out that several distinct electrical resistivity temperature dependencies were reported for single crystals of LaFeAsO grown in *a single batch* of molten KI flux.[20] This observation suggests that the semiconducting-like behavior observed in some samples is not a direct consequence of impurities unique to the method of synthesis employed in this work.

Electrical resistivity $\rho(T)$ data, measured on a single-crystalline sample of LaFeAsO under nearly hydrostatic applied pressures up to 2.6 GPa, are shown in Fig. 1. The semiconducting-like behavior of $\rho(T)$ persists through 2.6 GPa as is seen in Fig. 1. A prominent feature is observed in the $\rho(T)$ data, which is associated with the SDW order, and is clearly suppressed to lower temperature by increasing pressure. To more quantitatively resolve the transition temperature associated with the SDW phase transition, T_{SDW}, we have

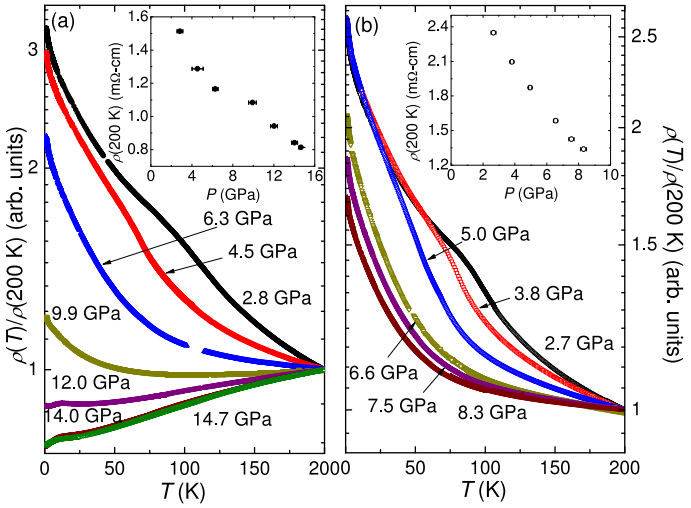

FIG. 2: Electrical resistivity ρ vs. temperature T on a semilog scale for two distinct samples of LaFeAsO using the Bridgman anvil cell technique from 2.7 GPa to 14.7 GPa. The data have been normalized by their value at 200 K. The inset in each panel shows the electrical resistivity values at 200 K for each pressure.

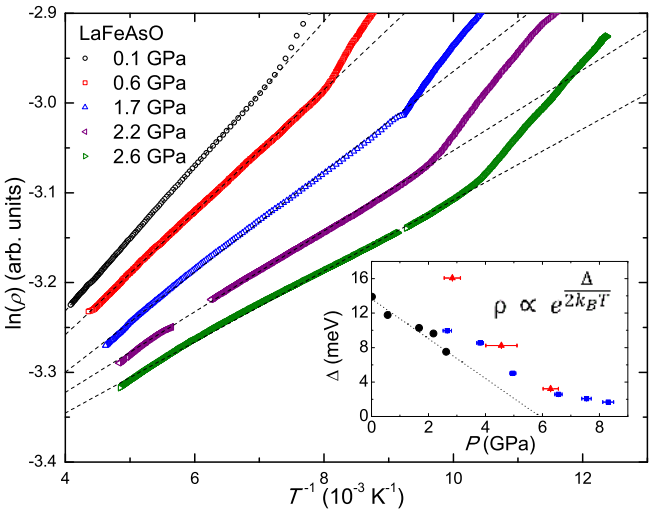

FIG. 3: Electrical resistivity ρ plotted as $\ln(\rho)$ vs. $1/T$. A linear fit to the data above the spin-density wave ordering temperature T_{SDW} shows that an Arrhenius law, $\ln(\rho) \propto (\Delta/2k_BT)$, may be used to estimate the energy gap Δ. The inset shows Δ for the samples measured in a piston-cylinder cell (PCC) (black solid circles), Bridgman anvil cell (BAC) (blue solid squares), and diamond anvil cell (DAC) (red solid triangles). The PCC results show a steady suppression of $\Delta(P)$ which extrapolates linearly to $\Delta = 0$ meV near 6 GPa. The results from the BAC and DAC measurements suggest $\Delta = 0$ meV at pressures near 10 GPa.

calculated the derivative of $\rho(T)$ with respect to temperature (displayed in the inset of Fig. 1). We identify the minima exhibited in these data with T_{SDW}.

The data displayed in Fig. 1 clearly demonstrate that T_{SDW} is monotonically suppressed with increasing pressures up to 2.6 GPa. To study what happens at higher pressures, we performed measurements in a Bridgman anvil cell (BAC) on two distinct samples (data displayed in Fig. 2). These data have been normalized by their values at 200 K, which are plotted in the insets of Fig. 2 as a function of pressure. Features associated with SDW order are also observed in these data at the lowest pressures, but are much broader and less distinct than the analogous features in Fig. 1, which is likely a consequence of the quasi-hydrostaticity of the BAC measurement technique. Despite this experimental detail, a clear and consistent picture emerges when we consider the data in Figs. 1 and 2, wherein SDW order appears to be suppressed with applied pressure. The suppression of SDW order has also been seen in studies of polycrystalline samples of LaFeAsO under similar conditions.[17]

For temperatures above T_{SDW} and T_{ST}, the semiconducting-like temperature dependence of the electrical resistivity of our samples can be fit using an Arrhenius law to estimate the energy gap Δ as a function of pressure. Along with the systematic suppression of T_{SDW}, the estimated gap decreases with increasing pressure as shown in Fig. 3. Studies of this kind have been performed on single crystals of LaMnPO wherein the pressure at which Δ reaches zero coincides with the emergence of metallic behavior.[32] Our study shows a similar suppression of Δ. The energy gap calculated from data taken in the nearly-hydrostatic cell extrapolates linearly to approximately 6 GPa; unfortunately, this pressure is beyond the limit of the piston cylinder cell. However, electrical resistivity measurements performed under quasi-hydrostatic pressure suggest that the energy gap vanishes near 10 GPa, which is consistent with the change in behavior of our single crystals from semiconductor-like to metallic behavior in those measurements. This can be seen in the data from measurements in a BAC (Fig. 2) as well as a DAC (Fig. 4). First principles calculations suggest the electronic density of states increases near 10 GPa, consistent with the transition to metallic behavior seen in our data.[33]

There are certainly considerable errors involved with estimating Δ by this method, and significant pressure gradients can develop during measurements utilizing a solid pressure medium, as in the BAC and DAC. Both of these issues probably play a role in producing the discrepancies in the $\Delta(P)$ values we obtain from measurements of LaFeAsO in nearly-hydrostatic and quasi-hydrostatic environments. However, despite the presence of some quantitative discrepancies, we observe a systematic suppression of the energy gap in data from measurements using all three techniques.

Electrical resistivity data collected using a DAC can be seen on a semi-log plot in Fig. 4. A crossover to a metallic temperature dependence occurs near 10 GPa as observed in the Bridgman cell data shown in Fig. 2. Additionally, we detected a low-temperature reduction in scattering reminiscent of the onset of superconductivity in the BAC data. Similar behavior has been observed in other studies where the onset of a superconducting transition attains values as high as 21 K at 29 GPa.[17,34,35] While we did not observe a complete transition to

zero resistance nor a systematic change in the temperature of the downturn T_D, we note that other studies on polycrystalline samples observed an incomplete low-temperature downturn at 1.5 GPa.[17] A full transition was observed only at 12 GPa using a cubic anvil cell, but not otherwise. This may suggest that higher pressures, or improved hydrostaticity could produce a full superconducting transition in our samples. Additionally, it is possible that polycrystalline samples studied previously contained oxygen deficiencies in the grain boundaries leading to incomplete transitions. Another study on single crystals grown from a KI flux revealed a low temperature downturn in electrical resistivity near 11 K.[20] Magnetization data suggested that this was related to a transition from AFM to FM order; however, the mechanism by which the application of pressure might induce such a magnetic transition in our samples is not clear.

The electrical resistivity data in Fig. 4 exhibit a feature at temperatures T^* above T_{SDW} that increases systematically with increasing pressure. The inset for Fig. 5 also clearly shows the evolution of T^* as pressure increases. A linear fit of $T^*(P)$, extracted from Fig. 4, yields $dT^*/dP \sim 1.8$ K/GPa. In an effort to understand the origin of this feature at T^*, we considered whether it may be identified as T_{ST}. A study of the thermal expansion of polycrystalline samples of LaFeAsO shows a feature in the coefficient of thermal expansion that corresponds to the structural transition at T_{ST}.[21] We are able to make a rough estimate of dT_{ST}/dP using the Ehrenfest relation and the magnitudes of the jumps at T_{ST} in measurements of specific heat[18] and the coefficient of thermal expansion,[21] and obtain a result on the order of 10^3 K/GPa. This result is considerably larger than the observed behavior for dT^*/dP, but they both share a positive pressure dependence. It is worth noting that our estimate of dT_{ST}/dP using the Ehrenfest relation is based on a mixture of results from both single crystals and polycrystalline samples; it would be more meaningful to perform a calculation of dT_{ST}/dP using jumps in data for the specific heat and the coefficient of thermal expansion that were measured on the same sample. X-ray diffraction measurements under applied pressure could be used to determine the boundary of the structural phase transition directly, and these experiments are currently underway. We note that a feature at T^* is not evident in the measurements performed in the piston-cylinder cell or the Bridgman anvil cell as shown in Fig. 1 and Fig. 2, respectively, even at similar nominal pressures. This is possibly a consequence of the varying degrees of hydrostaticity inherent in each technique. The measurements made using the PCC technique are significantly more hydrostatic than those made using steatite as a pressure transmitting medium (BAC and DAC techniques). In the DAC, the sample is compressed between quasi-hydrostatic solid steatite and a diamond anvil; in this environment the sample is likely to be substantially more strained than in the BAC.

A temperature-pressure phase diagram summarizing the results of this study is presented in Fig. 6. The phase diagram clearly shows the suppression of T_{SDW} with pressure up to 6 GPa, the low temperature downturn at T_D observed in the electrical resistivity measurements under quasi-hydrostatic pressure, and the feature at T^* observed in the DAC measurements. The suppression of T_{SDW} with pressure appears to be linear up to $\sim$ 6 GPa, which is in contrast to the positive curvature observed in the study on polycrystalline samples.[17]

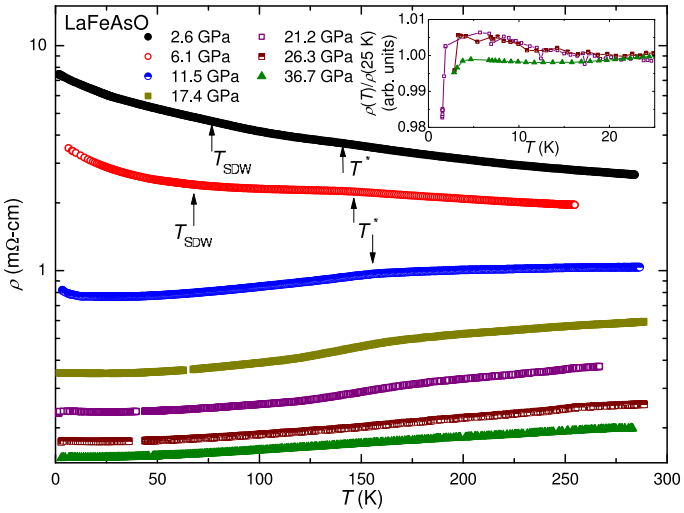

FIG. 4: Electrical resistivity ρ vs. temperature T measured using a diamond anvil cell from 2.6 GPa to 36.7 GPa. A metallic state is clearly induced near 11.5 GPa. We also note the evolution of a high-temperature feature at a temperature denoted as T^*. The inset shows $\rho(T)$ data normalized to their values at 25 K for measurements under applied pressure $P \geq 21.2$ GPa. A sharp low-temperature downturn is observed in each case.

The linear extrapolation of T_{SDW} to zero temperature, as shown in Fig. 6, assumes that the phase transition remains second order for all pressures. It is important to note that we were unable to resolve a feature associated with SDW order in Bridgman anvil cell data for pressures higher than $\sim$ 5 GPa (see Fig. 2). This could simply reflect the quasi-hydrostatic character of the pressure medium in those measurements and may mean that the feature has just broadened and is more difficult to resolve; however, given our results, we are not able to rule out the possibility that SDW order terminates in a first-order phase transition at some pressure higher than $\sim$ 6 GPa as happens in $LaFeAsO_{1-x}F_x$ at $x = 0.05$.[3]

It is interesting that the suppression of $\Delta(P)$, shown in the inset of Fig. 3, appears to correlate with the suppression of T_{SDW} (T_{SDW} extrapolates linearly to 0 K near 8 - 10 GPa) as this would suggest that the semiconducting-like behavior is likely an intrinsic quality of the as grown samples. The pressure range within which LaFeAsO evolves from semiconducting-like to a metallic temperature dependence appears as a grey region, which clearly distinguishes between the suppression of the SDW order at lower pressure and the emergence of the low-temperature downturn at higher pressures. This temperature-pressure phase diagram for single crystals of LaFeAsO is distinct from the phase diagram obtained from measurements on polycrystalline samples wherein superconductivity appears to emerge before SDW or-

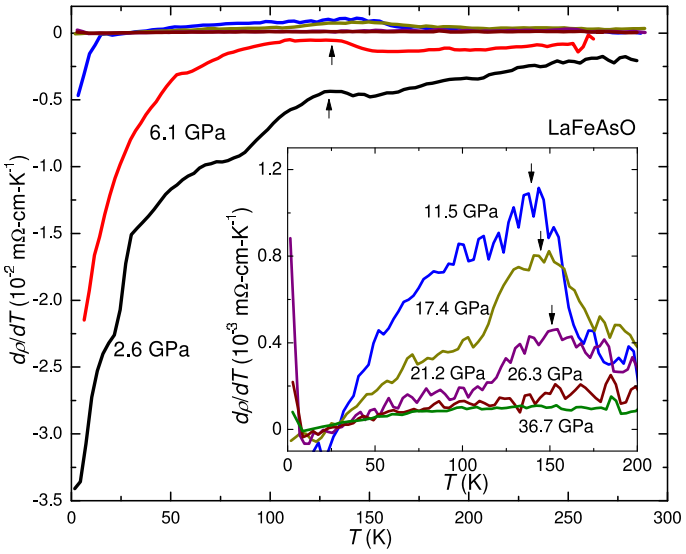

FIG. 5: The first derivative of the electrical resistivity ρ with respect to temperature T, $d\rho/dT$ vs T, measured in a diamond anvil cell. The $d\rho/dT$ data reveal a feature corresponding to spin-density wave order as well as an unexpected feature at higher temperature T^*. The inset emphasizes the feature at T^* in the data measured under applied pressures from 11.5 GPa to 36.7 GPa. It is clear that T^* increases with increasing pressure.

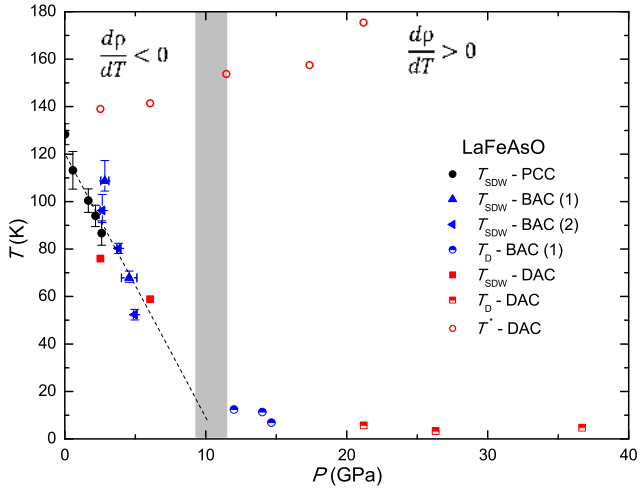

FIG. 6: Temperature-pressure ($T - P$) phase diagram for LaFeAsO summarizing the results of this study. T_{SDW} denotes the transition temperature of the spin-density wave order, while the low-temperature downturn, seen in the electrical resistivity data under high applied pressure, occurs at T_D. T^* separates regions where semiconducting-like behavior is observed for electrical resistivity ($d\rho/dT < 0$) from regions where metallic behavior ($d\rho/dT > 0$) is observed. The dashed line is a guide to the eye indicating the expected linear suppression of T_{SDW} to $T = 0$ K assuming the transition remains of second order for all pressures.

der is completely suppressed,[17] and suggests a strong competition between the conditions giving rise to SDW order and the possible superconducting phase which emerges at T_D.

The current experiment provides some insight into the interrelation between superconductivity and magnetism in the *Ln*FeAsO compounds, in particular, and Fe-pnictide compounds, in general. The substitution of elements such as F for O (or introduction of O vacancies), Th for *Ln*, and Co for Fe in *Ln*FeAsO (*Ln* = lanthanide) compounds dope the FeAs layers with electrons, suppress the SDW, and induce superconductivity with relatively high superconducting critical temperatures T_c ranging from $\sim$ 27 K for LaFeAsO to $\sim$ 56 K for SmFeAsO. For F substitution in LaFeAsO, the suppression of the SDW with F composition appears to be an abrupt first order transition in which the SDW region abuts the superconducting region with no overlap between the SDW and superconducting phases.[36] The chemical substitutions also produce disorder, but this has little effect on the superconductivity, which persists over a large range of F composition with a high value of T_c. In contrast, in the experiments on the LaFeAsO single crystals reported herein, the suppression of T_{SDW} with pressure is nearly linear and, presuming it remains of second order, extrapolates to a putative SDW quantum critical point (QCP) in the vicinity of 10 GPa. As noted above, the suppression of the energy gap Δ with pressure also extrapolates to 0 K in the vicinity of 10 GPa, above which metallic behavior is observed. Thus, it seems surprising that there is no evidence for superconductivity above 1 K, the low temperature limit of the present electrical resistivity measurements, near or above the critical pressure $\sim$ 10 GPa where T_{SDW} and Δ are suppressed toward 0 K. As noted above, high values of $T_c \approx 27$ K are achieved when the FeAs layers are doped with electrons by the F, O vacancy, Th, and Co substituents when their concentrations are sufficiently large to suppress the SDW. While the application of pressure closes the energy gap Δ in LaFeAsO, the charge carrier density in the resultant metallic state is apparently not large enough to induce high T_c superconductivity. Although the SDW transition is suppressed upon the application of pressure at a putative QCP near 10 GPa, the quantum fluctuations of the magnetic order parameter in the vicinity of the SDW QCP do not produce high T_c superconductivity in LaFeAsO. Interestingly, there are many examples of Ce-based heavy fermion f-electron compounds[37–40] in which superconductivity and non-Fermi liquid behavior in the normal state properties are observed near the critical pressure where AFM is suppressed toward 0 K (AFM QCP) which have been attributed to magnetic order parameter fluctuations. Electronic structure calculations may provide some insight into the differences in the effects of electron doping of the FeAs layers through chemical substitution and the application of pressure on the superconducting and normal state physical properties of LaFeAsO.

While there are very small down turns in the electrical resistivity of the LaFeAsO single crystals that occur above the presumed SDW QCP at $\sim 12 - 15$ GPa and are suggestive of the onset of superconductivity, the superconductivity would have to be associated with minute amounts of filaments of a superconducting phase, since the filaments would otherwise

form a complete circuit and lead to a sharp drop of the electrical resistivity to zero.[41,42] If these features are indeed due to filaments of a superconducting phase, it is not clear whether the phase is intrinsic or extrinsic.

In contrast, the experiments of Okada *et al.* [17] on polycrystalline samples of LaFeAsO under applied pressure indicate that superconductivity is induced under pressure in a wide dome with a maximum T_c of $\sim$ 22 K at about 12 GPa. However, the resistive transitions are very broad and the electrical resistivity only drops to zero at 12 GPa. In the polycrystalline sample of LaFeAsO, for which $T_N \approx 150$ K, the depression of T_N is linear up to $\sim$ 2 GPa and extrapolates to 0 K near 11 GPa. Above $\sim$ 2 GPa, the $T_c(P)$ curve bends away from this linear behavior with positive curvature and drops to a value of $\sim$ 80 K near 13 GPa, above which the SDW transition is no longer discernable in the resistivity measurements and without any indication of a QCP. This behavior of the polycrystalline samples may be due to their granular and inhomogeneous nature and oxygen deficiency at the grain boundaries, where the latter could be the source of the superconductivity, which only occupies a small volume of the sample. More extensive studies of both polycrystalline and single crystal specimens under pressure will be needed to achieve an understanding of these differences.

IV. CONCLUDING REMARKS

We have measured the electrical resistivity of single-crystalline samples of LaFeAsO under applied pressures up to ~ 36.7 GPa. The feature in the electrical resistivity associated with the onset of SDW order in these single-crystalline samples is more clearly resolvable under pressure compared to previous studies on polycrystalline samples. We observe a clear suppression of the SDW ordering temperature with pressure, with T_{SDW} extrapolating linearly to zero near 8 GPa (nearly hydrostatic measurements) or 10 GPa (Bridgman anvil cell measurements). Similar to some other reports on single and polycrystalline samples[2,19,20], the samples measured in this study exhibit a negative $d\rho/dT$ over a broad temperature range. By fitting the temperature-dependent electrical resistivity at each pressure, we have estimated the energy gap associated with the semiconducting-like behavior and found that $\Delta(P)$ decreases under applied pressure. For the measurements taken under nearly hydrostatic conditions, Δ extrapolates to zero at 6 GPa. The semiconducting-like temperature dependence of the electrical resistivity at low pressure evolves into metallic behavior where $d\rho/dT > 0$ near 10 GPa. The suppression of the SDW order, followed by the closing of the gap, and the transition to a metallic electrical resistivity is not accompanied by the appearance of bulk superconductivity; although, small downturns in the electrical resistivity, consistent with filamentary superconductivity, do appear in this pressure range. One explanation is that the slight downturns in electrical resistivity are associated with the superconductivity of small oxygen-deficient regions in the crystals. The superconductivity previously reported for polycrystalline samples of LaFeAsO under pressure could also be the result of oxygen-deficient regions of the sample, since it is known that oxygen deficiency gives rise to superconductivity in this material.

Preliminary X-ray diffraction measurements under pressure on polycrystalline samples of LaFeAsO show no structural phase transition from orthorhombic to tetragonal symmetry at 18 K up to 30 GPa.[43] The absence of a structural phase boundary appears to indicate a decoupling of T_{ST} from T_{SDW}, which is distinct from the case for fluorine substitution studies where the structural phase transition and SDW order remain closely coupled until the abrupt emergence of superconductivity. More comprehensive X-ray diffraction measurements on single crystals of LaFeAsO to track T_{ST} as a function of applied pressure would be very useful and are currently being carried out.

Acknowledgments

High-pressure research at University of California, San Diego was supported by the National Nuclear Security Administration under the Stewardship Science Academic Alliance program through the U.S. Department of Energy grant number DOE DE-NA0001841. Sample synthesis was supported by AFOSR-MURI Grant AFOSR FA 9550-09-1-0603, while physical properties characterization at ambient pressure was supported by the U.S. Department of Energy, Office of Basic Energy Sciences, Division of Materials Sciences and Engineering under Award Grant no. DE-FG02-04-ER46105. Lawrence Livermore National Laboratory is operated by Lawrence Livermore National Security, LLC, for the US Department of Energy (DOE), National Nuclear Security Administration (NNSA), under Contract No. DE-AC52-07NA27344. Y. K. V. acknowledges support from DOE-NNSA Grant No. DE-NA0002014.

* Current Address: Department of Physics, University of Florida, Gainesville, Florida 32611, USA

[1] Y. Kamihara, H. Hiramatsu, H. Masahiro, R. Kawamura, H. Yanagi, T. Kamiya, and H. Hosono, J. Am. Chem. Soc. **128**, 10012 (2006).

[2] Y. Kamihara, T. Watanabe, M. Hirano, and H. Hosono, J. Am. Chem. Soc. **130**, 3296 (2008).

[3] S. A. Kivelson and H. Yao, Nat. Mater. **7**, 927 (2008).

[4] D. C. Johnston, Adv. Phys. **59**, 803 (2010).

[5] P. M. Aswathy, J. B. Anooja, P. M. Sarun, and U. Syamaprasad, Supercond. Sci. Technol. **23**, 073001 (2010).

[6] G. R. Stewart, Rev. Mod. Phys. **83**, 1589 (2011).

[7] Q. Liu, X. Yu, X. Wang, Z. Deng, Y. Lv, J. Zhu, S. Zhang, H. Liu, W. Yang, L. Wang, et al., J. Am. Chem. Soc. **133**, 7892 (2011).

[8] M. Fu, D. A. Torchetti, T. Imai, F. L. Ning, J.-Q. Yan, and A. S. Sefat, Phys. Rev. Lett. **109**, 247001 (2012).

[9] M. A. McGuire, A. D. Christianson, A. S. Sefat, B. C. Sales, M. D. Lumsden, R. Jin, E. A. Payzant, D. Mandrus, Y. Lluan, V. Keppens, et al., Phys. Rev. B. **78**, 094517 (2008).

[10] D. K. Pratt, M. G. Kim, A. Kreyssig, Y. B. Lee, G. S. Tucker, A. Thaler, W. Tian, J. L. Zarestky, S. L. Bud'ko, P. C. Canfield, et al., Phys. Rev. Lett. **106**, 257001 (2011).

[11] M. D. Johannes and I. I. Mazin, Phys. Rev. B **79**, 220510 (2009).

[12] Q. Si and E. Abrahams, Phys. Rev. Lett. **101**, 076401 (2008).

[13] R. Pöttgen and D. Johrendt, Z. Naturforsch. B **63b**, 1135 (2008).

[14] J. Paglione and R. L. Greene, Nature Physics **6**, 645 (2010).

[15] J. Zhao, Q. Huang, C. de la Cruz, S. Li, J. W. Lynn, Y. Chen, M. A. Green, G. F. Chen, G. Li, Z. Li, et al., Nat. Mater. **7**, 953 (2008).

[16] S. Kitagawa, T. Iye, Y. Nakai, K. Ishida, C. Wang, G.-H. Cao, and Z.-A. Xu, J. Phys. Soc. Jpn. **83**, 023707 (2014).

[17] H. Okada, K. Igawa, H. Takahashi, Y. Kamihara, M. Hirano, H. Hosono, K. Matsubayashi, and Y. Uwatoko, J. Phys. Soc. Jap. **77**, 113712 (2008).

[18] C. A. McElroy, J. J. Hamlin, B. D. White, M. A. McGuire, B. C. Sales, and M. B. Maple, Phys. Rev. B **88**, 134513 (2013).

[19] J. Q. Yan, S. Nandi, J. L. Zarestky, W. Tian, A. Kreyssig, B. Jensen, A. Kracher, K. W. Dennis, R. J. McQueeney, A. I. Goldman, et al., Appl. Phys. Lett. **95**, 222504 (2009).

[20] A. Jesche, F. Nitsche, S. Probst, T. Doert, P. Müller, and M. Ruck, Phys. Rev. B **86**, 134511 (2012).

[21] R. Klingeler, L. Wang, U. Köhler, G. Behr, C. Hess, and B. Büchner, J. Phys. Conf. Ser. **200** (2010).

[22] P. Quebe, L. J. Terbüchte, and W. Jeitschko, J. Alloy Compd. **302**, 70 (2000).

[23] A. Ricci, N. Poccia, B. Joseph, L. Barba, G. Arrighetti, G. Ciasca, J. Q. Yan, R. W. McCallum, T. A. Lograsso, N. D. Zhigadlo, et al., Phys. Rev. B **82**, 144507 (2010).

[24] A. Jayaraman, A. R. Hutson, J. H. McFee, A. S. Coriell, and R. G. Maines, Rev. Sci. Instrum. **38**, 44 (1967).

[25] T. F. Smith, C. W. Chu, and M. B. Maple, Cryogenics **9**, 53 (1969).

[26] J. Wittig, Z. Phys. **195** (1966).

[27] B. Bireckoven and J. Wittig, J. Phys. E: Sci. Instrum. **21**, 841 (1988).

[28] A. Jayaraman, Rev. Mod. Phys. **55**, 65 (1983).

[29] T. S. McCauley and Y. K. Vohra, Appl. Phys. Lett. **66**, 1486 (1995).

[30] S. T. Weir, J. Akella, C. Aracne-Ruddle, Y. K. Vohra, and S. A. Catledge, Appl. Phys. Lett. **77**, 3400 (2000).

[31] A. D. Chijioke, W. J. Nellis, A. Soldatov, and I. F. Silvera, J. Appl. Phys. **98** (2005).

[32] J. Guo, J. W. Simonson, L. Sun, Q. Wu, P. Gao, C. Zhang, D. Gu, G. Kotliar, M. Aronson, and Z. Zhao, Sci. Rep. **3**, 2555 (2013).

[33] Y. Yang and X. Hu, J. Appl. Phys. **106** (2009).

[34] T. Kawakami, T. Kamatani, H. Okada, H. Takahashi, S. Nasu, Y. Kamihara, M. Hirano, and H. Hosono, J. Phys. Soc. Jpn. **78**, 123703 (2009).

[35] H. Takahashi, K. Igawa, K. Arii, Y. Kamihara, M. Hirano, and H. Hosono, Nature **453**, 376 (2008).

[36] H. Luetkens, H. H. Klauss, M. Kraken, F. J. Litterst, T. Dellmann, R. Klingeler, C. Hess, R. Khasanov, A. Amato, C. Baines, et al., Nat. Mater. **8** (2009).

[37] H. Hegger, C. Petrovic, E. G. Moshopoulou, M. F. Hundley, J. L. Sarrao, Z. Fisk, and J. D. Thompson, Phys. Rev. Lett. **84**, 4986 (2000).

[38] N. D. Mathur, F. M. Grosche, S. R. Julian, I. R. Walker, D. M. Freye, R. K. W. Haselwimmer, and G. G. Lonzarich, Nature **394**, 39 (1998).

[39] D. Jaccard, K. Behnia, and J. Sierro, Phys. Lett. A **163**, 475 (1992).

[40] I. R. Walker, F. M. Grosche, D. M. Freye, and G. G. Lonzarich, Physica C **282**, 303 (1997).

[41] H. Xiao, T. Hu, S. K. He, B. Shen, W. J. Zhang, B. Xu, K. F. He, J. Han, Y. P. Singh, H. H. Wen, et al., Phys. Rev. B **86**, 064521 (2012).

[42] S. W. Hsu, S. Y. Tsaur, and H. C. Ku, Phys. Rev. B **38**, 856 (1988).

[43] R. Kumar, J. Hamlin, Y. Xiao, S. Sinogeikin, P. Chow, B. Maple, Y. Zhao, and A. Cornelius, Bull. Am. Phys. Soc. **56** (2011).